4th MASHCON, Hamburg - Uliczka et al. (eds) - © 2016 Bundesanstalt für Wasserbau ISBN 978-3-939230-38-0 (Online)
DOI: 10.18451/978-3-939230-38-0_7

A NEW SLENDER BODY THEORY FOR SHALLOW WATER AND COMPARISON WITH EXPERIMENTAL AND TWO OTHER NUMERICAL METHODS

M Alidadi, University of British Columbia, Vancouver, Canada,
O Gören and **D B Danişman,** Istanbul Technical University, Istanbul, Turkey,
S Calisal, Piri Reis University, Istanbul, Turkey,

SUMMARY

This study compares the results of a new slender body formulation for shallow water applications with two other well established methods for a Wigley hull. For the slender-body method for shallow water, the velocity potential is decomposed into a double-body potential and a perturbation potential. Using an order of magnitude analysis, the three-dimensional governing equation for the flow field around a slender hull is reduced into a series of two-dimensional problems in cross-flow planes as in the 2D+t methods. An Eulerian-Lagrangian approach is then used to satisfy the free surface condition. An implicit unsteady solver modeling and VOF model are used for the CFD simulations, using Star-CCM+. The numerical results obtained from these two methods for a Wigley hull are then compared with the new results. In addition the wave elevation and wave resistance results are compared against the predictions of Dawson method and experimental data. The effect of shallow water on resistance trim and squat are calculated and a ceiling for speed in shallow water is observed.

NOMENCLATURE

B	Beam of a ship
CFD	Computational Fluid Dynamics
D	Draft of a ship
L	Length of a ship
V	Velocity of the ship (m/s)
Rw	Wave resistance (N)
P	Pressure (N/m^2)
g	Gravitational acceleration (m/s^2)
x, y, z	Coordinates as in figure 1.
n	Normal vector
t	Time (s)
η	Wave elevation (m)
Φ	A potential function
υ	kinematic viscosity (m^2/s)
ρ	Density of water (kg/m^3)

letter subscripts denote differentiation along that direction

1 INTRODUCTION

For decades the experimental testing has been the main tool for research and development in ship hydrodynamics. However this started to change with the improvements of computers since 1970's. Nowadays the computational tools are extensively used in hydrodynamics, as:

- Building and testing of a ship model is expensive.
- Numerical hydrodynamic studies of ship models are becoming cheaper and faster with improved software and hardware.
- Computational methods provide detailed, visual information about the flow field around the hulls.

Most of the early numerical methods such as Michel integral, 2D+t formulation [1] and Dawson methods [14] are based on the potential flow theory. They are fast and provide a relatively good estimation of wave resistance. As the potential flow methods do not take into account the viscosity, the viscous resistance is normally calculated using empirical methods. However in the past decades, CFD methods based on RANS simulations become more popular as the computational power improved. This paper is focused on comparing three numerical methods for ship hydrodynamics for shallow water. A new Slender-body method, an approach based on the Dawson algorithm and a CFD methodology are first explained. Then the wave profiles and wave resistance and shallow water effects are compared against the experimental values for a Wigley hull with principal dimensions Length L=2 m, Beam B=0.2 m and Draft D=.123 m.

2 NEW SLENDER–BODY FORMULATION

The Slender-body methods have been adopted extensively for flow calculation around slender hulls. Numerous researchers at the University of British Columbia did the ground breaking work for what is now called as 2D+t formulation in recent publications for wave pattern and resistance and vortex shedding of slender hulls (see [1, 2], [3], [4, 5]). Maruo and Song [6, 7] used this method to calculate the bow impact and deck wetness on a Wigley hull. Tulin and Wu [8] numerically calculated the divergent waves generated by a Wigley hull using a Slender-body method.

Development of the new Slender-body methods was a result of the desire to apply 2D+t method for shallow water and include some upstream influence in the calculations, assuming that such additions will be improving the results, especially for shallow water applications. This was done by including a double body potential explicitly in the formulation. Using an order of magnitude analysis, the three-dimensional flow problem is then converted into a series of two-dimensional problems which are easier to solve than the original problem.
The free-stream potential is taken as the base potential in the studies mentioned above. However at very low Froude numbers, the flow around a hull can be approximated by the flow around a double-body consisting of the submerged part of the hull and its image about mean free surface [9]. In the new Slender-body formulation presented here, the double-body potential is used as the base potential because it is considered to be a better representation of the actual flow potential than the free-stream potential especially at low Froude numbers and shallow water applications.

2.1 MATHEMATICAL FORMULATIONS OF THE SLENDER-BODY METHOD

The coordinate system for a ship moving at constant speed U through otherwise undisturbed water is shown in Figure 1. It is fixed on the ship with x and y axes on the waterline plane and the origin at amidships and on the center plane. The equation for the Wigley hull geometry in this coordinate system is:

$$y = Y(x,z) = \pm\frac{B}{2}\left(1-\frac{4x^2}{L^2}\right)\left(1-\frac{z^2}{D^2}\right) \qquad (Eq\ 1)$$

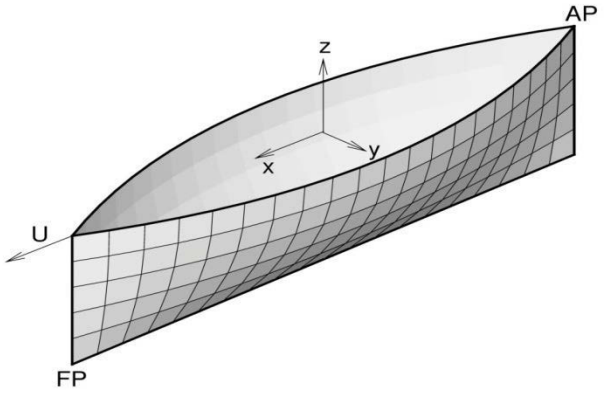

Figure 1. Coordinate system fixed to the hull

The fluid is assumed to be inviscid and incompressible and the fluid motion irrotational. The flow is represented by a velocity potential ψ which satisfies the Laplace's equation

$$\psi_{xx} + \psi_{yy} + \psi_{zz} = 0 \qquad (Eq\ 2)$$

The kinematic and dynamic boundary conditions for the steady free surface represented by $z = \eta(x,y)$ are:

$$\psi_x\eta_x + \psi_y\eta_y - \psi_z = 0 \qquad (Eq\ 3)$$

$$\frac{1}{2}\left(\psi_x^2 + \psi_y^2 + \psi_z^2 - U^2\right) + g\eta = 0 \qquad (Eq\ 4)$$

The impermeable boundary condition on the hull with normal vector $\boldsymbol{n}$ (positive pointing outwards) is

$$\psi_x n_x + \psi_y n_y + \psi_z n_z = 0 \qquad (Eq\ 5)$$

Next we assume that the velocity potential ψ is composed of a perturbation wave potential ϕ and the double-body potential $\bar{\phi}$, i.e.

$$\psi = \phi + \bar{\phi} \qquad (Eq\ 6)$$

where the double-body potential $\bar{\phi}$ satisfies Laplace's Equation 2), then the perturbation potential ϕ must satisfy Laplace's equation

$$\phi_{xx} + \phi_{yy} + \phi_{zz} = 0 \qquad (Eq\ 7)$$

Using an order of magnitude analysis for a slender hull (see Appendix A) and assuming that ϕ_{xx} is much smaller than $\phi_{yy}$and ϕ_{zz}, the governing equation 7 simplifies into :

$$\phi_{yy} + \phi_{zz} = 0 \qquad (Eq\ 8)$$

.

Equation 8 denotes that the flow around a slender hull can be seen as a two-dimensional problem in the cross flow planes along the x axis, which is easier to solve than the original three-dimensional problem (7). A sketch of a cross flow plane is shown in Figure 2.

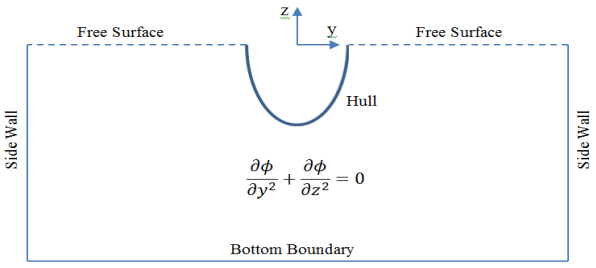

Figure 2. Sketch of a cross flow plane

An order of magnitude analysis of the individual terms in the free surface equations and hull boundary condition results in (see Appendix A) :

$$\left(\bar{\phi}_y + \phi_y\right)\eta_y - \left(\bar{\phi}_z + \phi_z\right) = 0 \qquad (Eq\ 9)$$

$$\frac{1}{2}\left(\bar{\phi}_x^2 + \bar{\phi}_y^2 + \bar{\phi}_z^2 - U^2\right) + \frac{1}{2}\left(\phi_y^2 + \phi_z^2\right) + \left(\bar{\phi}_y\phi_y + \bar{\phi}_z\phi_z\right) + g\eta = 0 \qquad (Eq\ 10)$$

$$\phi_y n_y + \phi_z n_z = -\left(\bar{\phi}_y n_y + \bar{\phi}_z n_z\right) \qquad (Eq\ 11)$$

The kinematic and dynamic boundary conditions are non-linear equations and are applied on the free surface at $z = \eta(x, y)$ which is unknown a priori. These equations were linearized by expanding them about the undisturbed free surface at $z = 0$. Since $\bar{\phi}_z = 0$ on the free surface, the free surface boundary conditions become:

$$\bar{\phi}_y \eta_y - \phi_z = 0 \qquad at\ z = 0 \quad (Eq\ 12)$$

$$\frac{1}{2}\left(\bar{\phi}_x^2 + \bar{\phi}_y^2 + \bar{\phi}_z^2 - U^2\right) + \bar{\phi}_y \phi_y + g\eta = 0 \quad \text{at z=0} \qquad (Eq\ 13)$$

Solving equation 8 in a cross flow plane requires specifying the boundary conditions on the side walls and at the bottom boundaries. Here they are assumed to be impermeable. For the calibration purposes of the new results the side walls are placed 30B away from the body in order to ensure the waves do not reflect into the computational domain. The bottom boundary is specified at various locations and for infinitely deep condition at $30D$ from the body to minimize the bottom effect.

2.2 SOLUTION APPROACH

The time-stepping approach developed by Longuet-Higgins and Cokelet [10] is used for the implementation of the Slender-body method. It involves a two-step procedure divided into an Eulerian boundary element method and a Lagrangian stepping procedure following particles.

2.2 (a) Boundary Element Method

The first step involves solving the two-dimensional Laplace Equation 8 in a cross flow plane using the body boundary condition and the velocity potential ϕ_0 known on the free surface from the previous time step. Applying Green's third identity to the Laplace Equation 8 gives an integral equation for the perturbation potential at a field point q in the cross flow plane (see [11] and [12])

$$\phi(q) = \frac{1}{2\pi}\int_S \left(\frac{\partial \phi}{\partial n}\ln r - \phi\ \frac{\partial}{\partial n}\ln r\right) ds \qquad (Eq\ 14)$$

Where r is the distance from a source point p to a field point q and S is the boundary for the cross flow plane.
In order to calculate the unknown boundary values, the boundary S is divided into a series of panels with constant singularity distributions. Applying boundary conditions to equation 14 gives the system of linear equations:

$$\sum_{j=1}^{N} A_{ij} \left.\frac{\partial \phi}{\partial n}\right|_j + B_{ij}\phi_j = 0 \qquad i = 1, \cdots, N \qquad (Eq\ 15)$$

Where N is the number of panels on the boundaries and coefficients A_{ij} and B_{ij} are defined as:

$$A_{ij} = \frac{1}{2\pi}\int_j \ln r\ ds\ ; B_{ij} = \frac{1}{2\pi}\int_j \frac{\partial}{\partial \mathrm{n}}\ln r\ ds \qquad (Eq 15-b)$$

The coefficient A_{ij} (B_{ij}) represents influence of a panel j with a source (doublet) distribution of unit strength on a panel i [12].

2.2 (b) Lagrangian –Eulerian method

The second step involves a Lagrangian method to calculate the perturbation potential and the free surface location at the next cross-flow plane. This marching from one cross-flow plane to the next one can be viewed as a time-domain problem with a time step:

$$dt = \frac{dx}{\bar{\phi}_x} \qquad (Eq\ 16)$$

where dx is the spatial step along the longitudinal axis. It is set to $dx = 0.001\ m$ in this study.

For obtaining the kinematic and dynamic boundary conditions in the Lagrangian form, the derivative is defined as:

$$\frac{d}{dt} = \bar{\phi}_y \frac{\partial}{\partial y} \qquad (Eq\ 16-b)$$

Therefore the kinematic and dynamic boundary conditions and in the Lagrangian form can be written as:

$$\frac{d\eta}{dt} = \Phi_x \quad at\ z = 0 \qquad (Eq\ 17)$$

$$\frac{d\phi}{dt} = \frac{1}{2}\left(U^2 - \left(\bar{\phi}_x^2 + \bar{\phi}_y^2\right)\right) - g\eta \quad at\ z = 0 \quad (Eq\ 18)$$

The Lagrangian form of the flow velocity in y direction then becomes:

$$\frac{dy}{dt} = \bar{\phi}_y \qquad (Eq\ 19)$$

Using the two step Adams-Bashforth method, the values for the perturbation potential and free surface location at a new cross flow plane are obtained as :

$$\eta(t + dt) = \eta(t) + \left(\frac{3}{2}\eta_t(t) - \frac{1}{2}\eta_t(t - dt)\right)dt$$
$$\phi(t + dt) = \phi(t) + \left(\frac{3}{2}\phi_t(t) - \frac{1}{2}\phi(t - dt)\right)dt$$
$$y(t + dt) = y(t) + \left(\frac{3}{2}y_t(t) - \frac{1}{2}y_t(t - dt)\right)dt \qquad (Eq\ 20)$$

where η_t, $\phi_t$and $y_t$are determined from equations 19.
The wave resistance R_w is calculated by integrating the pressure field over the still water hull surface:

$$R_w = \int_{-L/2}^{L/2} dx \int_{S_B} p \cdot n_x dA \qquad (Eq\ 21)$$

where S_B represents the girth of the hull section, and p is the pressure obtained from the Bernoulli's equation:

$$p = -\rho\left[U\phi_x + \frac{1}{2}\left(\phi_y^2 + \phi_z^2 + gz\right)\right] \qquad (Eq\ 22)$$

The wave resistance coefficient C_w is determined using the formulation:

$$C_w = \frac{R_w}{0.5\rho U^2 L^2} \qquad (Eq\ 23)$$

For the results presented in this paper, the starting cross section was at $L/4$ upstream of the bow. The perturbation potential and wave elevation values were set to zero on this cross section. We defined 75 panels on the free surface at the starting section. The size of these panels increased toward the impermeable wall in a geometric progression with the initial size $D/10$. We used 10 panels on the hull surface when the cross section intersects the hull.

2.3 CALCULATION OF DOUBLE-BODY POTENTIAL

The double-body potential is calculated using the boundary element method developed by Hess and Smith [13]. The governing equation for this potential is the three-dimensional Laplace equation

$$\nabla^2\overline{\phi} = 0 \qquad (Eq\ 24)$$

subject to the impermeable hull boundary condition

$$\nabla\overline{\phi}\cdot\boldsymbol{n} = 0 \qquad (Eq\ 25)$$

Similar to the methodology described above, the equation (Eq) is converted into a system of linear equations

$$\sum_{j=1}^{M} C_{ij}\sigma_j = \boldsymbol{U}\cdot\boldsymbol{n} \quad for\ i = 1,\cdots,M \qquad (Eq\ 26)$$

where M is the number of quadrilateral panels on the hull surface and its image around the undisturbed free surface, and σ_j is the source strength of a panel j. The coefficient C_{ij} obtained from the relation

$$C_{ij} = \frac{1}{4\pi}\int_j \nabla\left(\frac{1}{r}\right).ndS \qquad (Eq\ 26-b)$$

and represents effect of a source panel j with unit strength on a panel i [12].
The double-body potential is calculated in this study using 50 panels in the x direction and 20 panels in the z direction.

3 DAWSON METHOD

Hess and Smith developed a boundary element method in 1967 for computing the flow around a submerged body in an infinite domain [13]. Dawson modified this method in 1977 for a surface-piercing body. One may refer to the thesis by Raven for a comprehensive explanation on this method [14].

The theoretical essence of Dawson method is based on the low-Froude-number theory. Similar to the method explained in the previous section, the total velocity potential is decomposed into a double-body and a perturbation potential (see equation 6). The double-body potential $\overline{\phi}$ is regarded as a "slowly varying potential" and hence its derivatives are of the order of (U). Newman [15] showed that the perturbation potential ϕ = O(ε^2) and wave elevation $\eta = O(\varepsilon)$ with $\varepsilon \equiv U^2/2g \ll 1$. In another study Calisal et al. showed that η = O(Fr^2) which is parallel to Newman's finding [16]. Based on this analysis the kinematic and dynamic free surface conditions are combined into a single linearized equation with respect to ϕ:

$$\nabla\overline{\phi}\cdot\nabla\left[-(\nabla\overline{\phi})^2 + \nabla\overline{\phi}\cdot\nabla\phi\right] + \frac{1}{2}\nabla\phi\cdot\nabla(\nabla\overline{\phi})^2 + g\phi_z = 0 \quad \text{at } z = 0 \qquad (Eq\ 27)$$

By adopting the definition of derivatives along a streamline, Dawson expressed the above equation as

$$\left(\overline{\phi}_l^2\phi_l\right)_l + g\phi_l = 2\overline{\phi}_l^2\overline{\phi}_{ll} \quad at\ z = 0 \qquad (Eq\ 28)$$

where

$$\overline{\Phi}_l = |\nabla\overline{\Phi}\ \ | = \sqrt{\overline{\Phi}_x^2 + \overline{\Phi}_{ly}^2} \qquad (Eq\ 28-b)$$

The potential flow problem is now reduced into solving the three dimensional Laplace equation $\nabla^2\overline{\phi} = 0$ subject to boundary conditions $\overline{\phi}_n = 0$ on the body and free surface condition 28. The radiation condition is fulfilled in this method by a 4-point backward differentiation scheme. The implementation of this method involves distributing panels on the plane z = 0 and on the hull surface as shown in Figure 3. The solution is then obtained by employing the Hess and Smith's method which uses source panels with constant strength. The wave elevation and pressure in this method are calculated from equations:

$$\eta = \frac{1}{2g}\left[U^2 + \overline{\phi}_l^2 - 2\overline{\phi}_l\phi_l\right] \qquad (Eq\ 29)$$

$$p = -\frac{\rho}{2}\left[U^2 + (\nabla\overline{\phi})^2 - 2\nabla\overline{\phi}\cdot\nabla\phi\right] \qquad (Eq\ 30)$$

The wave resistance is also computed by integrating the pressure over the hull surface (see equation 22).

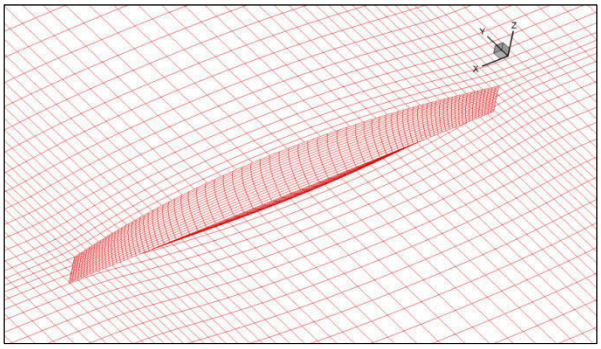

Figure 3. Distribution of panels on the hull and free surface

4 CFD METHOD

The usage of Computational Flow Dynamics (CFD) based on RANS equations is rapidly increasing for marine applications due to the improvements of computers. Here we implemented the CFD method for the Wigley hull by conducting simulations in the Star-CCM+ software. The corresponding coordinate system is at amidships on the undisturbed free surface (see Figure 1). As the hull is symmetric about its center plane of symmetry, only half of it is considered in the simulations. The domain based on hull length L extends from:

- *3.5L* to *-6.5L* in longitudinal direction
- *1L* to *-3L* in vertical direction
- *0* to *3L* in lateral direction

The applied boundary conditions are:

- Symmetry plane at the hull centerplane.
- Symmetry plane at the side of domain
- Hydrostatic pressure corresponding to undisturbed water surface at the outlet boundary
- Inlets with prescribed velocity and volume fraction at the upstream, top and bottom boundaries

The mesh used contains 372212 hexahedral cells. In order to obtain accurate results, we used local refinements and prism layers along the wetted surface of hull. The calculations used a mesh structure on the hull surface and the symmetry plane. In addition we had mesh at the still water level with refinements in the wake region. An implicit unsteady solver with k-omega turbulence modeling and VOF wave's model is used for simulations. The time step is set based on the inlet velocity from the equation:

$$\mathrm{dt} = \frac{\mathrm{L}}{50\mathrm{U}} \qquad (Eq\ 31)$$

5 VALIDATION IN DEEP WATER

One of the main objectives of this study is to estimate the shallow water effects on the sinkage and trim of a ship. A critical and the target case is the sailing of tankers in Vancouver harbor Canada . For these reasons an existing formulation that is 2D+t method is modified and a formulation suitable for shallow water studies is developed. The new code is first tried for deep water studies of the resistance, waterline profile. Once validated the code is then used for finite depth conditions.

Comparisons of different numerical calculations are reported below. The methods described above are implemented for the Wigley hull with dimensions given at section 1.

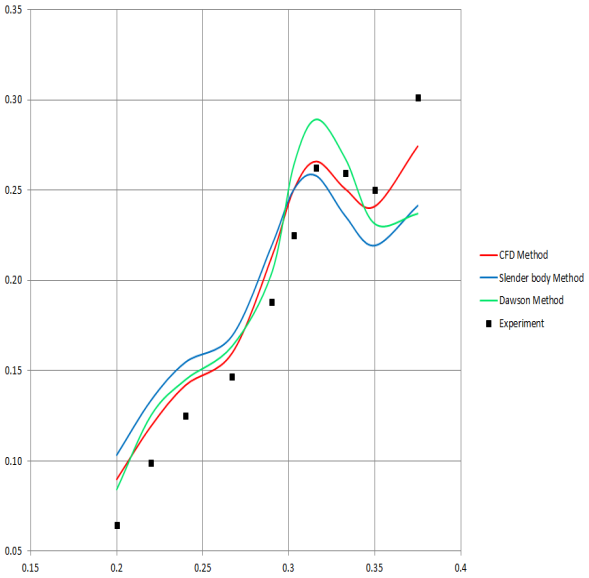

Figure 4. Comparison of numerical wave resistance coefficients with Dawson, new formulation and experimental values

The new code is validated with using the results of other codes for resistance and wave profile first. The general agreement of the resistance prediction with the new formulation with experimental resistance data could be considered as acceptable Figure (4). This is in view of the dispersion of such data coming from different towing tanks. Aanesland [18] gave averaged values from towing tank databases where the Wigley hull was towed fixed and free to trim and squat. Aanesland's numerical results were obtained by a three dimensional linear potential flow formulations similar to Dawson's method. However Kelvin sources were distributed in the outer domain to satisfy wave radiation conditions.

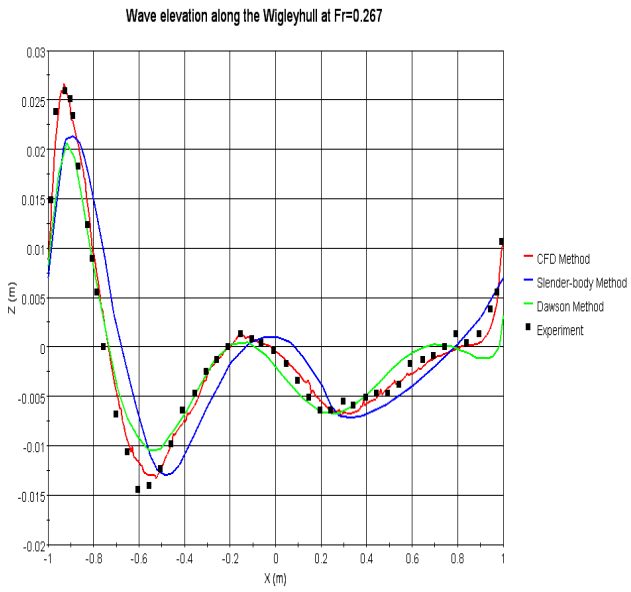

Figure 5. Wave elevation on the Wigley hull side at Fr= 0,267

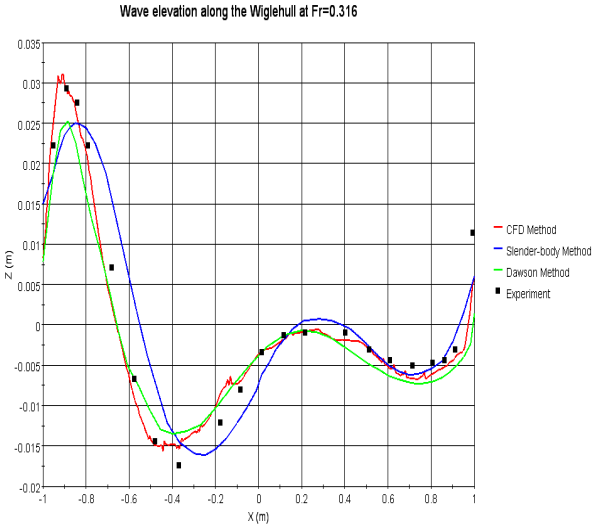

Figure 6. Wave elevation on the Wigley hull side at Fr=0,316

Figure 5 and Figure 6 show the comparison of the wave profiles along the hull at Froude numbers F_R=0.267 and F_R=0.316. The experimental results for F_R=0.267 are from a testing at the department of Naval Architecture and Ocean Engineering at the Yokohama National University [17], while the results for F_R=0.316 are obtained by Maruo and Song from tests on a 6-meter Wigley hull model [6]. The wave profiles of the CFD method are in a good agreement with experiments at both Froude numbers. The CFD predictions for the position and magnitudes of the wave peaks and troughs have a good match with the experimental results. On the other hand, the wave profiles for the Slender-body and Dawson methods have similar trends to the experiments; however there are some discrepancies between them and experimental values, especially around the bow section. The first wave peak is underestimated by both of the potential flow methods which might be due to linearization of the free surface boundary conditions. Also, the Dawson method has a better prediction of the location of wave peaks and troughs than the Slender-body method. This is possibly a result of the order of magnitude analysis used in the development of the Slender-body method. A new way for the start of the calculation is to be implemented soon.

6 FINITE DEPTH EFFECTS

Figure 7 shows that the depth effect for resistance is significant as the depth Froude number increases. Similarly the figure 6 shows that that the trim increases significantly with depth Froude number while the squat coefficient remains almost constant.

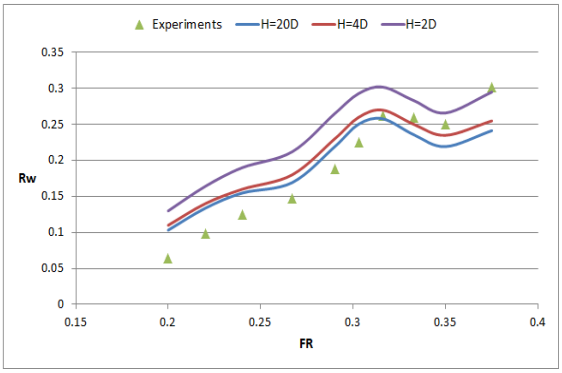

Figure 7. Wave making resistance deep and shallow water comparisons with new formulation compared to averaged experimental values of Aanesland

The results for wave resistance with the new formulation with finite depth or shallow water are reported in figure 7. The shallow water effect becomes significant as the clearance becomes smaller. Deep water sinkage and trim values by the 2D+t method are by Wong and Calisal [5] and shown in Figure 8. Sinkage is nondimensionalized with $U^2/2g$ and trim is given as a percentage of the ship length. the results are then compared with averaged values reported by Aanesland [18]. The nondimensional sinkage calculated by the 2D+t method is in good agreement with the experimental data however it seems to underestimate at higher Froude numbers. In contrast the trim is over estimated in the Froude number range of 0.27 to 0.35. The trim and squat in shallow water at relatively high Froude number with the new formulation are reported in Figure 9 and 10.

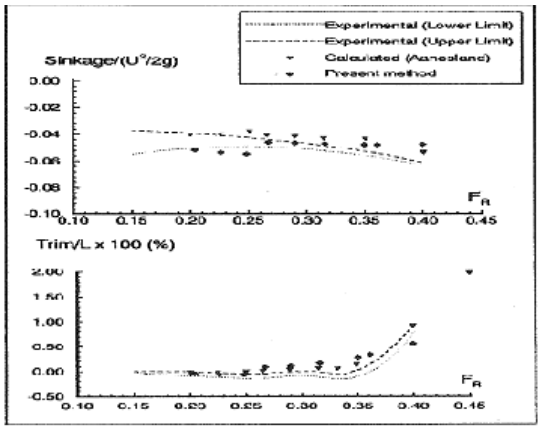

Figure 8. Computed and measured trim and sinkage for Wigley hull deep water with 2D+t formulation

The sinkage and trim angle are calculated assuming the Wigleyhull has a weight eqaul to 10.3 kgf. The pressure distribution is first obtained from the Bernoulli's equation. Then the hull sinkage by is calculated by balancing the hull weight with the hydrodynamic force in the vertical direction. The trim angle is similarly calculated by balancing the hull moment around the y-axis with the y-moment of hydrodynamic forces.

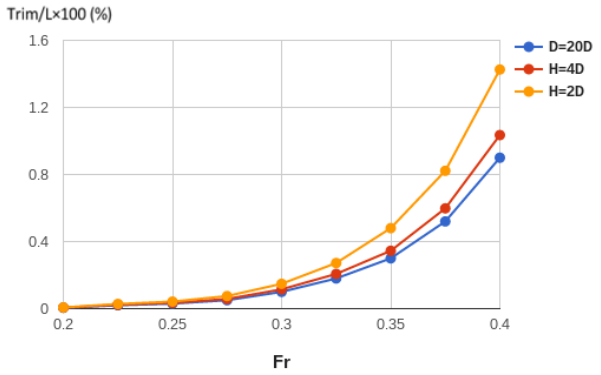

Figure 9. Computed trim variation with new formulation in shallow water with ship Froude number

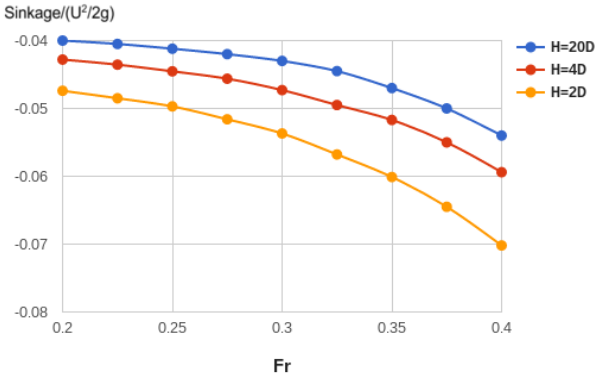

Figure 10. Water depth and Froude number effect on squat for Wigley hull with new formulation.

7 CONCLUSIONS

A new slender body formulation and two existing numerical methods for ship hydrodynamics were compared with the experimental values available for Wigley hull. The New Slender-body and Dawson methods, which are based on the potential flow theory, were easier and faster to implement than the CFD method. However the CFD method, which is based on RANS equations, had the best agreement with the experimental values in the validation in deep water. The CFD method was able to predict the magnitude and location of the wave peaks and troughs more accurately than the potential methods. The CFD results for wave resistance coefficients were also a better match with experimental values than the results obtained from Slender-body and Dawson methods. Some numerical challenge was faced as poor convergence when the depth Froude number is close to 1. A ceiling of ship operational speed is seen as the sinkage and trim increases with increasing speed. Application to shallow water of the new Slender body is expected to improve the earlier results reported above.

8 REFERENCES

1. Calisal, S.M.; Chan, J.L.K. (1989). A numerical calculation for ship bow wave, Ship Research, vol. 33, no. 1, p. 21–28.

2. Calisal, S.M.; Chan, J.L.K. (1993). A numerical procedure for time domain nonlinear surface wave calculations, Ocean Engineering, vol. 20(1), pp. 19-32.

3. Allievi, A.; Calisal, S.M. (1993). A semi-implicit, semi-lagrangian finite element model for nonlinear free surface flow. 6th International Conference on Ship Hydrodynamics.

4. Wong, L.H.; Calisal, S.M. (1994). A numerical solution for potential flows including the effects of vortex shedding, J. Offshore Mech. Arct. Eng. 115(2): pp. 111-115.

5. Wong, L.H.; Calisal, S.M. (1996). Numerical algorithms for slender bodies with vortex shedding and density stratification, Ship Research, vol. 40, no. 1.

6. Maruo, H.; Song, W.-S. (1990). Numerical appraisal of the new slender ship formulation in steady motion, Proceedings of the 18th Symposium on Naval Hydrodynamics, Michigan, pp. 239-256.

7. Song, W.-S.; Maruo, H. (1993). Bow impact and deck wetness: simulation based on nonlinear slender body theory, Proceedings of the 3rd International Offshore and Polar Engineering Conference, Singapore.

8. Tulin, M.; Wu, M. (1996). Divergent bow waves, 21th Symposium on Naval Hydrodynamics, p. 661-679, Trondheim.

9. Faltinsen, O.M.(2005). Hydrodynamics of High-Speed Marine Vehicles, Cambridge University Press.

10. M. S. Longuet-Higgins and E. D. Cokelet, (2005). The Deformation of Steep Surface Waves on Water. I. A Numerical Method of Computation. Proceedings of Royal Society London, vol. 350, pp. 1-26.

11. Brebbia, C.A.; Dominquez, J. (1992). Boundary Elements: An Introductory Course, WIT Press.

12. Katz, J.; Plotkin, A. (2001). Low-Speed Aerodynamics, Cambridge University Press.

13. Hess, J. L.; Smith, A.M.O. (1981). Calculation of potential flow about arbitrary bodies, Progress in Aerospace Sciences, vol. 8, pp. 1-138, 167.

14. Raven, H.C. (1996). A solution method for the nonlinear ship wave resistance problem, PhD Thesis, Technische Universiteit Delft, The Netherlands.

15. Newman, J.N. (1976). Linearized wave resistance theory, Proceedings of the International Seminar on Wave Resistance, p. 31-34, Tokyo.

16. Calisal, S.M.; Goren, O.; Okan, B. (1991). On an iterative solution for nonlinear wave calculations, Journal of Ship Research, vol. 35, no. 1, pp. 9-14.

17. Hayashi, K.; Kunishige, Y. (1988). *Measurement of wave pattern around a yawed ship model*, Graduation Thesis, Yokohama National University, Japan

18. Aanesland V. (1989). A Hybrid Model for Calculating wave Making resistance, *Proceedings of the Fifth International Conference on Numerical Ship Hydrodynamics*, Japan, pp. 657 -666.

9 AUTHORS' BIOGRAPHIES

Mahmoud Alidadi holds a PhD degree in mechanical engineering from University of British Columbia (UBC). As a research fellow at UBC, he worked on development a numerical method for studying hydrodynamics of slender ships.

Ömer Gören received his Ph.D. degree in 1985 from ITU and was then post-doctoral fellow at UBC in 1986-87. Since then he has been a faculty at ITU Dept. of Naval Architecture and Marine Eng. His focus of reserach interests are free surface hydrodynamics and hull shape optimization for resistance.

Devrim Bülent Danışman received his Ph.D. degree in 2004 from ITU. Subsequently, he worked as research fellow at the University of Newcastle during 2000-2001. Currently he is an Assoc.Prof. at ITU. His field of interests are computational and experimental resistance analysis and form optimization.

Sander Calisal did his doctoral work at U Cal Berkeley with late professor J.V. Wehausen and has worked in USNA and UBC Canada and is a professor at Piri Reis University. He researched on ship hydrodynamics and ship design.

10 APPENDIX A: ORDER OF MAGNITUDE ANALYSIS

Replacing the potential ψ from Equation 6 in the kinematic and dynamic boundary conditions Eq. 3 and Eq. 4 gives

$$\left(\overline{\phi}_x + \phi_x\right)\eta_x + \left(\overline{\phi}_y + \phi_y\right)\eta_y - \left(\overline{\phi}_z + \phi_z\right) = 0$$

$$\frac{1}{2}\left(\left(\overline{\phi}_x + \phi_x\right)^2 + \left(\overline{\phi}_y + \phi_y\right)^2 + \left(\overline{\phi}_z + \phi_z\right)^2 - U^2\right) + g\eta = 0 \qquad \text{(A1-A2)}$$

Similarly the hull boundary condition 5 changes to

$$\phi_x n_x + \phi_y n_y + \phi_z n_z = -\left(\overline{\phi}_x n_x + \overline{\phi}_y n_y + \overline{\phi}_z n_z\right) \qquad \text{(A3)}$$

In order to simplify the above equations, non-dimensionalized variables are defined:

$$\tilde{x} = \frac{x}{L} \qquad \tilde{y} = \frac{y}{B} \qquad \tilde{z} = \frac{z}{D}$$

The order of magnitude of the individual terms in the governing equation 8 and boundary conditions A1-A3 are:

$$\phi_{xx} = O\left(\frac{\phi}{L^2\tilde{x}^2}\right) \quad \phi_{yy} = O\left(\frac{\phi}{B^2\tilde{y}^2}\right) \quad \phi_{zz} = O\left(\frac{\phi}{D^2\tilde{z}^2}\right)$$

$$\phi_x = O\left(\frac{\phi}{L\tilde{x}}\right) \quad \phi_y = O\left(\frac{\phi}{B\tilde{y}}\right) \quad \phi_z = O\left(\frac{\phi}{D\tilde{z}}\right)$$

$$n_x = O\left(\frac{n}{L\tilde{x}}\right) \quad n_y = O\left(\frac{n}{B\tilde{y}}\right) \quad n_z = O\left(\frac{n}{D\tilde{z}}\right)$$

$$\eta_x = O\left(\frac{\eta}{L\tilde{x}}\right) \quad \eta_y = O\left(\frac{\eta}{B\tilde{y}}\right)$$

$$\overline{\phi}_x = O\left(\frac{\overline{\phi}}{L\tilde{x}}\right) \quad \overline{\phi}_y = O\left(\frac{\overline{\phi}}{B\tilde{y}}\right)$$

One can conclude that for a slender hull where $O(D) \approx O(B)$ and $B/L \ll 1$

$$\phi_{xx} \ll \phi_{yy}, \phi_{zz} \qquad \phi_x\eta_x \ll \phi_y\eta_y$$

$$\phi_x^2 \ll \phi_y^2, \phi_z^2 \qquad \phi_x n_x \ll \phi_y n_y, \phi_z n_z$$

$$\overline{\phi}_x\eta_x \ll \overline{\phi}_y\eta_y \qquad \overline{\phi}_x\phi_x \ll \overline{\phi}_y\phi_y$$

$$\overline{\phi}_x n_x \ll \overline{\phi}_y n_y, \overline{\phi}_z n_z$$